Shotgun proteomics of peach fruit reveals major metabolic pathways associated to ripening

Ricardo Nilo-Poyanco
Universidad Mayor Facultad de Ciencias
Carol Moraga
Universite Claude Bernard Lyon 1
Gianfranco Benedetto
Universidad Andres Bello
Ariel Orellana
Universidad Andres Bello
Andréa Miyasaka Almeida (andrea.miyasaka@umayor.cl)
Universidad Mayor

Research article

Keywords: Fruit ripening, proteome, Rosaceae

Posted Date: April 16th, 2020

DOI: https://doi.org/10.21203/rs.3.rs-20851/v1

Version of Record: A version of this preprint was published on January 6th, 2021. See the published version at https://doi.org/10.1186/s12864-020-07299-y.

Abstract

Background

Fruit ripening in *Prunus persica* melting varieties involves several physiological changes that have a direct impact on the fruit organoleptic quality and storage potential. By studying the proteomic differences between the mesocarp of mature and ripe fruit, it would be possible to highlight critical molecular processes involved in the fruit ripening.

Results

To accomplish this goal, the proteome from mature and ripe fruit was assessed from the variety O'Henry through shotgun proteomics using 1D-gel (PAGE-SDS) as fractionation method followed by LC/MS-MS analysis. Data from the 131,435 spectra could be matched to 2,740 proteins, using the peach genome reference v1. After data pre-treatment, 1,663 proteins could be used for comparison with datasets assessed using transcriptomic approaches and for quantitative protein accumulation analysis. Close to 26% of the genes that code for the proteins assessed displayed higher expression at ripe fruit compared to other fruit developmental stages, based on published transcriptomic data. Differential accumulation analysis between mature and ripe fruit revealed that 15% of the proteins identified were modulated by the ripening process, with glycogen and isocitrate metabolism, and protein localization overrepresented in mature fruit, as well as cell wall modification in ripe fruit. Potential biomarkers for the ripening process, due to their differential accumulation and gene expression pattern, included a pectin methylesterase inhibitor, a gibbellerin 2-beta-dioxygenase, an omega-6 fatty acid desaturase and an ACC oxidase. These genes would be regulated by transcription factors enriched in zinc finger and GAGA-binding transcriptional activator protein domains.

Conclusions

Shotgun proteomics is an unbiased approach to get deeper into the proteome allowing to detect differences in protein abundance between samples. This technique provided a resolution so that individual gene products could be identified. Many proteins likely involved in cell wall and sugar metabolism, aroma and color, change their abundance during the transition from firm to soft fruit.

Background

Prunus persica (L) Batsch is one of the most economically important fruit crops in the Rosaceae family, with a broad climate distribution, relatively high yield and around 1,000 cultivars produced worldwide (Cao et al., 2014, Monti et al., 2016). *P. persica* has also become a very important plant model given its compact, small (227.3 Mb) and publicly accessible genome (Verde et al., 2017), the availability of homozygous doubled haploids, and its taxonomic proximity to other important fruit species such as apricot (*P. armeniaca*), plum (*P. salicina*), almond (*P. dulcis*) and apple (*Malus domestica*) (Aranzana et al., 2019).

Fruit ripening is a complex process that involves changes at multiple biochemical and physiological levels which impacts gene expression (Giovannoni et al., 2017), proteins and metabolites abundance (Monti et al., 2016, Wu et al., 2016). It is the last step of the broader process of fruit development, where the fruit increases in volume and the endocarp undergoes a hardening process, enclosing the seed in a secondary lignin-rich cell wall. During ethylene-dependent ripening, fruits transit from a photosynthetically active organ into an organ where the photosynthetic machinery is dismantled, carotenoids, sugars, organic acids and volatile compounds are accumulated, and the cell wall is loosed (Gapper et al., 2013). Overall, this conversion makes the fruit attractive for consumption as a rich source of fibers, vitamins and antioxidants, as well as its flavor, color and aroma.

Peach fruit ripening has been characterized at the molecular level in processes such as volatile and aroma production (Sánchez et al., 2013, Wang et al., 2016, Zhang et al., 2017), ethylene and other hormone biosynthesis and signaling (Tadiello et al., 2016, Wang et al., 2017), cell wall dismantling (Trainotti et al., 2003), pigments biosynthesis (Cao et al., 2017a, Cao et al., 2017b), and organic acids and sugars metabolism (Famiani et al., 2016, Vimolmangkang et al., 2016, Monti et al., 2016, Desnoues et al., 2018). *P. persica* transcription factors (TFs) involved in anthocyanin induction (Bianchi et al., 2015, Cao et al., 2017b), and ethylene biosynthesis (Bianchi et al., 2015, Wang et al., 2017) have also been characterized. Transcriptomic studies in *P. persica* have been used to improve the understanding of the molecular processes that underlie fruit chilling injury (Pegoraro et al., 2015, Pons et al., 2016, Nilo-Poyanco et al., 2019), and have not focused on fruit ripening.

Given the above, knowledge is still lacking about how peach fruit ripening is orchestrated at the molecular level. Proteome is a highly dynamic model for understanding the biological processes in an organ. Two-dimensional gels followed by mass spectrometry (MS) analysis have been the most frequent approach to evaluate changes in the proteome of fruits undergoing ripening. However, this approach is limited by the low numbers of proteins of interest identified, co-migration of proteins within the same spot, the absence of hydrophobic proteins, the expertise required to generate high quality 2D-gels and the extended time required to perform the images assessment and statistical analysis (Abdallah et al., 2012, Gapper et al., 2014).We propose that a 1D-gel followed by LC/MS-MS analysis proteomics approach based on a robust experimental and statistical framework can provide information regarding pathways and biological processes that are crucial for peach fruit ripening. Through this technique we could expand the number of proteins identified during the transition from mature to ripen fruit. The variety selected was O'Henry, since it is a proteome and transcriptome characterized melting peach variety (Nilo-Poyanco et al., 2010, 2012), which is the parental to several new-varieties.

Results

Mature and ripe mesocarp peach fruit proteomes differ greatly between amongst themselves and with other fruit developmental stages

The transition from mature into ripe fruit entails major changes in the fruit mesocarp firmness, titratable acidity, total soluble solids and respiration rate; and more subtle changes in ethylene biosynthesis (Campos-Vargas et al., 2006). To get a deeper insight into the proteins that are involved in this transition, a 1D SDS-PAGE gel followed by MS analysis was performed (Fig. 1). Data was then analyzed using MASCOT and Scaffold to focus on those proteins identified at a high confidence and to retrieve abundance data from these proteins in a format that is robust for downstream quantitative statistical analysis (Fig. 1, **Supplementary Fig. 1**). At first, a total of 131,435 spectra could be matched to 2,740 proteins, using the peach genome reference v1. After data cleaning from proteins spuriously identified or with an inadequate number of replicates, a total of 1,663 proteins were thus included in this study, representing a 6.2% of the *P. persica* primary transcripts proteome (**Supplementary Table 1**).

In order to check if the proteome represented by these 1,663 proteins had some bias in terms of its physicochemical composition, protein properties such as length, molecular weight, charge, protein stability, and hydrophobicity profiles were compared to the *P. persica* primary transcripts proteome (26,873 proteins) and to a similar sized 977 proteins set, extracted from juicy and mealy fruit mesocarp from the Spring Lady variety (Monti et al., 2019). In terms of data location, results indicated that for most of the parameters selected, the three populations have similar mean values (**Supplementary Table 2, Supplementary Fig. 2**), with the most substantial differences being related to charge and hydrophobicity, using the Guy scale (Guy HR, 1985). In terms of data dispersion, the *P. persica* primary transcripts proteome displayed a higher dispersion for 5 of the 6 parameters assessed, when compared to the datasets from the current proteome and the proteome from Spring Lady (**Supplementary Table 2, Supplementary Fig. 2**).

The functional analysis of the 1,663 proteins identified in this work, performed using Gene Ontology (GO) analysis, indicated that this protein set was enriched in processes related to carboxylic acid metabolism and intracellular transport, and to a lesser extent to protein folding (Fig. 2A).

We next asked if the genes encoding the proteins present in the mesocarp of mature and ripe fruits were more expressed at this stage, or if they were expressed at the same levels in any developmental stage of the fruit development. In order to answer this question, a contrast between the transcriptional expression was performed of 18,074 *P. persica* genes (herein “full-dataset”, variety Fantasia, GEO dataset GSE71561) at 125 days after full bloom (DAFB) against its expression at 41, 54, 69, 83, 111 DAFB. Close to 32% of the “full-dataset” did not display any expression level difference when contrasting its expression at 125 DAFB, corresponding to ripe fruit stage against any other stage (first lane, dark bar, Fig. 2B). This proportion was 5.9%, when considering the protein-coding genes assessed in this study (1,136 genes that matched our dataset, herein “proteomics-dataset”, first lane, grey bar, Fig. 2B). When assessing the number of genes that displayed its highest expression levels at 125 DAFB (second lane, Fig. 2B), 14.6% of the “full-dataset” displayed this behavior, compared to 25.8% of the “proteomics-dataset.” Finally, when assessing the number of genes that displayed its lowest expression levels at 125 DAFB (third lane, Fig. 2B), 14.1% of the “full-dataset” displayed this behavior, compared to 17.6% of the “proteomics-dataset”. This result indicates that an important proportion of the protein-coding genes characterized in

the mesocarp of the mature-ripe fruit reached their highest expression levels at the ripening stage of the peach fruit developmental curve.

Similar to the previous analysis, we evaluated if the protein-coding genes expressed at the fruit mesocarp during the fruit ripening were mainly expressed at this tissue or if they had an even expression across leaves, immature and ripe fruit. Therefore, a transcriptomic dataset derived from the variety Babygold, consisting of 20,149 genes, whose expression was characterized by means of RNA-seq at leaves, 2 cm immature and ripe fruit mesocarp (Fig. 2C, Lü et al., 2018), was assessed. Gene expression at leaves was characterized by close to 35% of the genes being more expressed at this tissue, compared to 16% in the current “proteomics-dataset.” Gene expression in immature fruit displayed 38% of the genes being more expressed at this tissue, whereas in the “proteomics-dataset” this number was of 29%. Finally, at ripe fruit, 26% of the genes displayed a higher expression in this tissue, whereas in the “proteomics-dataset” this number doubled to 52%. This result indicates that half of the protein-coding genes characterized in the mesocarp of the mature-ripe fruit reached their highest expression in ripe fruit.

Proteomic differences between mature and ripe fruits points to the mature fruit as the main stage in which sugar metabolism is modulated in the fruit mesocarp

Principal component analysis (PCA) was used as a diagnostic plot and to identify the main variables that explain the proteomic differences between the samples assessed. PCA was performed using the 1,663 proteins identified in all mature (O1) and ripe (O2) fruit samples assessed in this study. The principal component 1 (PC1) segregates mature from ripe fruit, explaining close to 34% of the variance associated to the samples, a high value considering that the samples used were biological replicates harvested from field grown trees (Fig. 3A). In fact, the second component could explain close to 23% of the variability and was likely associated with differences among fruits.

Quantitative changes between mature and ripe fruit proteome were assessed using a t-test after centering, normalizing and scaling the data to achieve a close to normal distribution (Methods section, **Supplementary Fig. 1**). Mature and ripe fruit displayed 52 and 22 proteins with a qualitative upregulation, and 88 and 86 proteins with a quantitative upregulation, respectively. Overall, 248 (14.9%) of the proteins identified in this study displayed a differential abundance between mature and ripe fruit (**Table 1**). A functional enrichment analysis of the proteins with a differential abundance was performed using Gene Ontology (GO). Proteins more abundant in mature fruit were associated to glycogen and isocitrate metabolism, and protein localization (Fig. 3B). No enrichment in any of the three GO sub-ontologies was found for proteins more abundant in ripe fruit. In terms of the chromosome distribution of the gene coding for these differentially accumulated proteins, the set differentially accumulated in mature fruit was enriched in chromosome 3; whereas the set differentially accumulated in ripe fruit was enriched in chromosome 6 (Fig. 3C). No enrichment was found after assessing all 1,663 proteins identified in this study.

Among the most relevant pathways associated to proteins with differential accumulation in mature fruit, there were several that could have a direct impact in the fruit organoleptic quality: Sucrose and sorbitol

conversion into fructose 6-phosphate (PWY-3801), raffinose and stachyose (PWY-5337), phenylacetaldehyde (PWY-5751), farnesyl diphosphate (PWY-5123) and glutamine (PWY-6549) biosynthesis (Fig. 4A, panels I to V). In ripe fruit, we selected the ethylene (ETHYL-PWY) and linoleoyl-CoA (PWY-6001) biosynthesis pathways (Fig. 4B, panels I and II). Proteins related to cell wall disassembly were also differentially accumulated in ripe fruit (Fig. 4B, panel III). Transport reactions, such as sorbitol transport, would also be upregulated in ripe fruit (Prupe.8G101200, **Table 1**).

Almost all steps of the gluconeogenesis pathway (GLUCONEO-PWY) were represented by proteins characterized in this study (Fig. 4C), indicating that the pathway was active in both stages. There were very few differences in the accumulation of the proteins between mature and ripe fruit. However, subtle differences were found including the step that interconverts glycerone phosphate (DHAP) into D-glyceraldehyde 3-phosphate (EC 5.3.1.1) and the step that converts oxaloacetate into phosphoenolpyruvate (EC 4.1.1.49), with higher accumulation levels in mature and ripe fruit, respectively.

In terms of regulatory pathways, the signaling cascade that leads to the ethylene biosynthesis inhibition through the action of brassinosteroids over kinases such as the serine/threonine-protein kinase BSK (Prupe.6G065600) and the receptor-like protein kinase FERONIA (Prupe.6G295900) was well represented in our mature fruit dataset (Fig. 4D).

Potential biomarkers of peach fruit ripening include cell wall modifying proteins and proteins involved in plant hormone biosynthesis

In order to determine which protein-coding genes could be used as biomarkers to differentiate between mature and ripe fruit stages, gene expression data across six developmental stages in fruit seeds and mesocarp, was plotted as heatmaps (Fig. 5, **Supplementary Fig. 3A**). An optimal biomarker would be a gene whose expression is low at any stage and tissue, but that achieves maximum expression in the mesocarp of a ripening tissue. When considering protein-coding genes from mature fruit (Fig. 5A), only two proteins came close to displaying this pattern, a raffinose synthase (RAFS, Prupe.6G032400) and an endoglucanase (ENDOGL, Prupe.5G118000, Fig. 5C). When considering protein-coding genes from ripe fruit (Fig. 5B), this pattern was mainly displayed by seven protein-coding genes, six of which were clustered. These six clustered genes included three cell wall modifying proteins (polygalacturonase, Prupe.4G262200; pectin methylesterase inhibitor, Prupe.1G114500; and protein trichome birefringence-like 41, Prupe.4G157600), the main peach fruit 1-aminocyclopropane-1-carboxylate oxidase (Prupe.3G209900), an omega-6 fatty acid desaturase (Prupe.7G076500), and a thaumatin (Prupe.3G144100). The seventh protein was a gibberellin 2-beta-dioxygenase (Prupe.1G111900). Interestingly, several of these proteins were consistently found to be more abundant in mesocarp of O'Henry ripe fruit using 2D-gel electrophoresis (**Supplementary Table 1, Supplementary Fig. 4, Nilo-Poyanco et al., 2012**). It is also interesting to note that, based on gene expression clusters, the "developmental stage" would be more relevant in terms of coordinating gene expression, than "tissue specificity" (**Supplementary Fig. 3A**).

Protein-coding genes involved in fruit ripening are potential targets for transcriptional factors enriched in NAC and SANT/Myb domains

The analysis of transcription factors (TFs) that had over-represented targets in the set of differentially accumulated proteins in mature and ripe fruit indicated that these two protein sets were regulated by different families of TFs. Ninety-four, 37 and 45 TFs were found to possess over-represented targets among the 1,663 protein-coding genes assessed in this study, among those differentially accumulated in mature fruit and among those differentially accumulated in ripe fruit, respectively (Fig. 6A). An analysis of the TF protein domains indicated that these three sets of TFs have different domain composition (Fig. 6B). The analysis was also extended to those TFs that targeted protein-coding genes with high expression in ripe fruit (identified as “Cluster”, see Fig. 4E), in order to find possible TFs that could be involved in triggering high gene expression.

Discussion

Proteomic approaches, based on 1D electrophoresis followed by MS (Fig. 1), have been successfully used to better understand fruit ripening in Rosaceae family species such as apricot (**D'Ambrosio et al., 2013**) and strawberry (Bianco et al., 2009). This approach has the great advantages of being among the most robust pipelines for proteomic analysis (**Fang et al., 2010**) and being able to capture hydrophobic proteins. Conversely, 2D electrophoresis approaches lack the presence of hydrophobic proteins due to protein precipitation in the IPG matrix (Molloy et al., 1999). Considering that the physicochemical properties of *P. persica* primary transcripts' proteome were similar to those of the proteome analyzed in the present study (**Supplementary Table 2, Supplementary Fig. 2**) and that low abundant proteins, such as TFs, could be detected in our dataset, the current analysis seems to truly reflect the fruit proteome, but with a bias in terms of primarily representing proteins with average physicochemical properties (**Supplementary Fig. 2**).

When compared to proteins extracted from ripening *P. armeniaca*, using 1D SDS-PAGE gel followed by MS, 76% of the 245 proteins identified in mature/ripe apricot fruit were also identified in mature/ripe peach fruit (D'Ambrosio et al., 2013), indicating that the proteins found in peach fruit mesocarp are characteristic of Prunus fruit. Further analysis using transcriptomic datasets reinforced this assertion (Fig. 2). In order to take full advantage of the proteins characterized in systems such as ripe fruit, it is important to follow a robust pipeline of MS analysis and protein quantification, to increase the confidence in the identifications performed and to support differential accumulation analysis. MS analysis was performed using a stringent cutoff for both peptide and protein match. Next, protein quantification was performed using the average total ion chromatograms (Average TIC, **Asara et al., 2008**) followed by pre-treatment data to get a data distribution as close to normal as possible (**Supplementary Fig. 1**), data scaling and centering, and data cleaning, to keep only those proteins that had a proper number of replicates to perform a statistical analysis of differential accumulation. All these steps explain the drop from 2,740 detected proteins to 1,663 assessed proteins. It is also worth to remember that label-free quantification, such as the one used in this work, is a good choice for proteomic

analysis that seeks to characterize as many unbiased proteins as possible. However, variations are higher than in techniques that rely on labeling, since in label-free quantification samples are individually prepared and comparison occurs later, during data analysis (**Lindemann et al., 2017**). In addition, variability among fruits in the field can be very high, even if the fruits were manually selected based on size, color and physicochemical parameters. Therefore, in many cases a protein may vary widely between different conditions, and its abundance variation due to biological and technical issues might hurdle the ability to identify this protein as differentially accumulated.

The fruit mesocarp proteome identified in this work (1,663 proteins) was functionally related to carboxylic acid metabolism, intracellular transport and protein folding (Fig. 2A). Transport proteins were mainly related to carbohydrates, ions, and vesicle-mediated transport (**Supplementary Table 1**), with very few transporters differentially accumulated. Protein folding, in turn, was mainly related to chloroplast chaperonins (Zhao and Liu, 2018). Both sets point to a fruit mesocarp with active cellular compartment transport and protein folding.

Mature and ripe fruit stages are the last in the fruit developmental curve, making it possible to compare protein-coding genes from our dataset with datasets that characterized ripening-related genes in *P. persica* (GEO dataset GSE71561 and Lü et al., 2018). Protein-coding genes expressed in mature/ripe fruit seemed to be time and tissue-specific, given that close to 25% peak their expression levels in ripe fruit when compared to other developmental stages, and 52% peaked their expression in ripe fruit mesocarp, compared to other tissues (Fig. 2B and 2C). Fruit-specific genes that displayed the strongest differentiation between peach and almond (*P. dulcis*) were also the most highly expressed, pointing to a functional specialization of protein-coding genes that are highly expressed in fruit (Velasco et al., 2016). Our results point to the same behavior in functionally specialized fruit proteins, i.e., proteins with high accumulation in fruit could be particularly involved in metabolism.

Samples and protein abundance differences between mature and ripe fruit mesocarp were striking, with a PCA first component splitting both samples and 14.9% of the assessed differentially accumulated proteins (Fig. 3A, **Table 1**). This reinforces the notion that mature and ripe fruits are different not only in terms of metabolic profiles, but also at the proteome level. Processes triggered in the mature fruit would be directed to glycogen and isocitrate metabolism, and protein localization (Fig. 3B), whereas a manual inspection indicated that protein-driven cell wall modification was much more represented in ripe fruit than in mature fruit (eight versus two proteins, **Table 1**, Fig. 4B). Seven of these cell wall proteins have been experimentally shown to be ethylene responsive: polygalacturonase (PG) Prupe.2G300900 (Qian et al., 2016), PpPG21 (Prupe.4G261900, Wang et al., 2019, Qian et al., 2016), PpPG22 (Prupe.4G262200, Trainotti et al., 2003, Qian et al., 2016, Hayama et al., 2006), beta-galactosidase (Prupe.3G050200, Trainotti et al., 2003), pectin methylesterase inhibitor (Prupe.1G114500, Zhu et al., 2017), expansin 3 (Prupe.6G075100, Hayama et al., 2006), and endo-1,4-beta-glucanase PpEG1 (Prupe.5G131300, Trainotti et al, 1997), highlighting the relevance of ethylene as a ripening promoting hormone in peach fruit of the melting variety. In addition, protein-coding genes from PpEG1, PpPG21, Prupe.2G300900 and Prupe.3G050200 belonged to the same gene cluster with higher expression in ripe fruit compared to

mature fruit, in the white flesh fast-melting peach “Hu Jing Mi Lu” (HJ, Li et al., 2015), pointing to a conserved mechanism of cell wall dismantling in peach fruits with a different genetic background.

Key processes involved in the organoleptic changes that occur in the transition from mature to ripe fruit

The ripening process involves changes in the fruit mesocarp flavor, color, aroma, and texture that have a direct impact on the fruit organoleptic quality. By studying the proteomic changes that are triggered during ripening, it would be possible to underscore some of the critical molecular processes involved in this transition. During this research, proteins involved in hormone, soluble sugars, organic acids, lipids and specialized metabolism were correlated with this transition, and their possible role in fruit ripening is discussed below.

Hormone Metabolism

There is multiple evidence that the plant hormone ethylene is involved in the regulation of the ripening process in climacteric fleshy fruit. Upon binding to its receptors, ethylene’s signal is propagated to several downstream components which in turn target promoters of many ethylene-inducible genes, directly involved in the dramatic changes that occur during the transition from mature to ripe fruit (Wang et al., 2019). The ACC synthase (ACS) and ACC oxidase (ACO) enzymes are responsible for turning S-Adenosyl methionine (SAM) into ethylene. In peach, the abundance of the ACO isoform ACO1 (Prupe.3G209900) transcript and protein correlates very closely with fruit ripening (Ruperti et al., 2001, **Trainotti et al., 2006, Nilo-Poyanco, 2012**). In this work, ACO1 also displayed a similar pattern, being more abundant in ripe fruit than in mature fruit (**Table 1**, Fig. 3D), validating the physiological characterization of the mature and ripe fruit stages at the molecular level.

The possible signaling cascades that modulate ethylene biosynthesis in climacteric fruit are poorly understood. Recently, in apple (*Malus × domestica*) and tomato (*Solanum lycopersicum*), both climacteric fruits, Feronia-like receptor kinases (FERLs) were shown to act as negative regulators of fruit ripening by inhibiting ethylene production (Jia et al., 2017). In the current study, a *P. persica* FERL (Prupe.6G295900), with over 75% of identity with the apple MdFERL1 and the tomato SlFERL1, was characterized as more abundant in mature than in ripe fruit (**Table 1**). In addition, upstream key regulators of FERL, such as BSK and BSU (Ren et al., 2019), were also more abundant in mature than in ripe fruit. This pattern suggests that this signaling pathway could regulate ethylene biosynthesis during peach fruit ripening, as its downregulation in the transition from mature to ripe fruit is correlated with the increase in ethylene biosynthesis in ripe fruit.

Sugar Metabolism

The sugar alcohol sorbitol is the main metabolite used to mobilize photosynthesis-derived carbohydrates from leaves to fruits in Rosaceae (Wei et al., 2014), being highly correlated with fruit taste and aroma (Cirilli et al., 2016), and of great interest for fruit breeders given its nutritional and sweetener qualities (Cantín et al., 2009). At a molecular level, sorbitol modulation could impact fruit quality by affecting

sugar-acid balance and starch accumulation (**Teo et al., 2006**). How this effect is generated is not clear, but it is postulated that sorbitol is catabolized in the cytosol, being the main driver of structural compounds biosynthesis and respiration in the peach fruit (Desnoues et al., 2018). In mature fruit, sorbitol could be used to generate fructose, which in turn could be metabolized into fructose 6-phosphate (F6P), by the enzyme fructokinase (Prupe.1G196700), which is differentially accumulated at this stage (Fig. 4B). F6P can be used to synthesize sucrose, the predominant soluble sugar in mature fruit, or enter the glycolytic pathway (Cirilli et al., 2016). In ripe fruit, the putative sorbitol transporter (SOT) Prupe.8G101200 accumulated more than in mature fruit (**Table 1**). This protein is a close homologue to candidate SOTs in pear (PbSOT19/21, **Yu et al., 2019**), apple (SOT6, Fan et al., 2009) and sour cherry (*P. cerasus*, PcSOT1, Gao et al., 2003). SOTs are represented by an expanded gene family in apple and peach (**Verde et al., 2013**), which is made up of 16 genes in *P. persica*. The ones that display the highest expression at the ripening stage were Prupe.8G101200 (PpePOL5, Nuñez et al., 2019) and Prupe.3G071100 (**Supplementary Fig. 3B**). Thus, the PpePOL5 transporter could be partially responsible for an increase in sorbitol content in ripe fruit of the O'Henry variety, compared to mature fruit (Guizani et al., 2019).

An intriguing question still under debate is what is the role of stored malate in fruit metabolism during the ripening process, as malate synthesis and not dissimilation is detected throughout ripening (Famiani et al., 2016). Malate levels are mainly regulated by its synthesis due to cytosolic carboxylation of phosphoenolpyruvate (PEP), its degradation due to decarboxylation also in the cytosol or by the conversion of tri- and dicarboxylates in the mitochondria, glyoxysome or cytosol (Etienne et al., 2013). Malate can be used as a sugar precursor through gluconeogenesis, to help regulate nitrogen metabolism (Famiani et al., 2016), as well as valves to balance metabolic fluxes given their function in indirect transport of reducing equivalents (**Hebbelmann et al., 2012**). According to the proteomic profiles assessed in this study, malate would be catabolized by the gluconeogenesis process to different metabolites in mature and ripe fruit (Fig. 4). In mature fruit, the differential accumulation of the protein triosephosphate isomerase would point to a preferred catalysis of malate to glyceraldehyde 3-phosphate, a triose phosphate that can be oxidized into pyruvate, providing the mature fruit with ATP and NADH. In ripe fruit, the differential accumulation of the enzyme phosphoenolpyruvate carboxykinase would help to keep the appropriate physicochemical conditions for the use of glutamate as nitrogen source for the biosynthesis of amino acids required at this stage (Famiani et al., 2016).

Among the soluble sugars present in the peach fruit, sucrose, fructose and glucose do not change much during the transition from mature to ripe fruit; in contrast to xylose, fucose and raffinose, according to an assessment of 15 *P. persica* varieties (**Monti et al., 2016**). In the current analysis, two key enzymes involved in raffinose biosynthesis (raffinose and stachyose synthases, **Table 1**, Fig. 4A) were more accumulated during the mature stage, indicating that in the O'Henry variety this metabolite accumulation would occur at the mature stage. Raffinose is an important metabolite given its antioxidant properties and role in stress tolerance (**Monti et al., 2016**).

Starch biosynthesis and accumulation is believed to happen at the early stages of fruit development, followed by its consumption until almost undetectable levels at maturity (Cirilli et al., 2016). However, enzymes involved on starch biosynthesis, such as 1,4-alpha-glucan-branching enzyme (SBE, Prupe.1G354000) and Glucose-1-phosphate adenylyltransferase small subunit (APS1, Prupe.3G192600) were still detected in mature fruit, with a drop in their levels in ripe fruit (Fig. 3C). SBE was also detected by others in the mesocarp of ripe peach fruits (**Jiang et al., 2020**), indicating that starch biosynthesis could still be active at later stages of fruit development. Another interesting fact is the differential accumulation of the atypical cysteine/histidine-rich thioredoxin 4 *P. persica* homologous (ACHT4, Prupe.7G001600, 64% identical) in ripe fruit. ACHT4 has been characterized in *A. thaliana* as a molecular switch of APS1, being able to quench APS1 activity (Eliyahu et al., 2015). By combining decreased accumulation of SBE and APS1 with an increase of ACHT4, the ripe fruit metabolism could downregulate starch content at this final developmental stage.

Fruit Aroma And Lipid Metabolism

Among the many dozens of volatiles peach fruits can produce, the γ- and δ-decalactones, C6 aldehydes and alcohols, terpenoids and volatile esters are the ones that are mainly related to fruit aroma (Zhang et al., 2010, Sánchez et al., 2013, Cao et al., 2019). Volatile esters are the product of alcohol acyltransferase-mediated biosynthesis, and degradation through carboxylesterase (CXE) activity (Cao et al., 2019). In tomato, low ester levels, which positively correlate with fruit liking, were associated to the enzyme SlCXE1 (**Goulet et al., 2012**). In peach, the carboxylesterase PpCXE1 (Prupe.8G121900) was shown to be able to degrade volatile acetate esters (Cao et al., 2019). In the present study, two CXE proteins were found to be more abundant in mature fruit than in ripe fruit, Prupe.1G439300 and Prupe.8G121500. The genes coding for these proteins were top-7 and top-8 in expression level in ripe fruit, among 19 putative CXEs in *P. persica* (Cao et al., 2019). Prupe.1G439300 is the best homologue to the tomato SlCXE1 (Cao et al., 2019) and its protein-coding gene displayed a peak of expression in ripe fruit (GEO dataset GSE71561), being a good candidate for further characterization.

Fruits can synthesize lactones that attract feeders for seed dispersal, mostly the γ-lactones decano-4-lactone and/or dodecano-4-lactone (**Schöttler and Boland, 1996**). These compounds, which primarily derive from oleic acids or derivatives, are metabolized by a series of enzymes, including epoxide hydrolases, to generate lactones such as undecano-4-lactone (**Schöttler and Boland, 1996**). They can be found both in fruit skin as well as mesocarp (Zhang et al., 2010). According to our data, lactone metabolism would also be differentially regulated in mature and ripe fruit, due to preferential accumulation of epoxide hydrolase EPH2 (Prupe.7G162300, Pirona et al., 2013) in mature fruit. On the other hand, the SRK2C kinase (Prupe.6G192200), which has been correlated to lactones using QTL analysis (**Sánchez et al., 2014**), is exclusively found in ripe fruit (**Table 1**). The target of SRK2 is unknown, and given its high expression (GEO dataset GSE71561), differential accumulation during the ripening process (**Table 1**), and correlation with lactone biosynthesis, it becomes an interesting candidate for further characterization.

Fruit ripening has been characterized as a senescing process, with cell membrane deterioration being the hallmark. Phospholipase D (PLD) is among the most relevant proteins involved in cell membrane deterioration in ripening fruits, acting upon phospholipids to generate phosphatidic acid (PA) and a free head group (Jincy et al., 2017). PLD action is also able to trigger a myriad of cellular processes, and therefore its activity is tightly regulated (Qin et al., 2002). PLDs have been grouped into five classes (α, β, γ, δ and ζ) according to several parameters such as domain structure and biochemical properties. Similar to most plant PLDs, PLDδ requires Ca^{2+} and is stimulated by phosphatidylinositol 4,5-bisphosphate (PIP2) (Qin et al., 2002). However, *Arabidopsis* PLDδ displays a distinctive property, which is to be activated by oleic acid (Qin et al., 2002). A peach PLDδ (Prupe.7G17540) was found to be more abundant in mature fruit than in ripe fruit (**Table 1**).

Fatty acid desaturase 1 (FAD1, Prupe.7G076500), a ω-6 Oleate desaturase (Sánchez et al., 2013), displayed increased abundance in ripe fruit (Fig. 4B, panel II), a pattern similar to the one displayed by its transcript in the *P. persica* Yulu variety (Zhang et al., 2010), in the GSE71561 dataset, and by its closest orthologue in *Fragaria vesca* (Sánchez-Sevilla et al., 2014). FAD1 gene expression was also sensitive to the ethylene signal transduction pathway inhibitor 1-methylcyclopropene (1-MCP), a compound known to negatively affect peach fruit aroma (Cai et al., 2019). This increase could imply that FAD1 could be involved in linoleic and linolenic acids biosynthesis in ripe fruit, in a similar way to its best homologue in *Arabidopsis thaliana* (AtFAD2, Zhang et al., 2010), or could be involved in γ-decalactone biosynthesis, as proposed for the *F. vesca* FaFAD1 (Sánchez-Sevilla et al., 2014).

Solute Transport

Aquaporins are transmembrane proteins that enable water and small neutral solute translocation across cellular membranes. Among the different types of aquaporins, those located in the vacuolar membranes are called tonoplast intrinsic proteins (TIPs). TIPs are classified into five groups (TIP1-5), and are able to transport hydrogen peroxide and glycerol, in addition to water (Regon et al., 2014). The *P. persica* aquaporin TIP1-1 (Prupe.7G125900) was found to be more abundant in ripe than in mature fruit mesocarp (**Table 1**). A close homologous (93% identity) protein-coding gene from sweet cherry (*P. avium*) was among the three most expressed aquaporins in the fruit, being mainly expressed in mesocarp throughout fruit development (Chen et al., 2019). The *P. persica* PpTIP1-1 transcriptional pattern was very similar (GEO dataset GSE71561), with the gene being expressed at a regular level throughout mesocarp development. This indicates that both Prunus TIP1-1 aquaporins conserved their tissue localization and expression patterns. Moreover, it indicates that these aquaporins could be key to transport water across the vacuole in the *Prunus* fruit mesocarp (Chen et al., 2019).

Conclusions

We have identified more than 1,500 proteins with high confidence using 1D SDS-PAGE fractionation associated to MS-MS detection. The differentially accumulated proteins in mature and ripe fruit identified in this study showed a high correlation with previous transcriptome studies. Differentially accumulated

proteins were mainly related to the metabolism of hormones such as ethylene and brassinosteroids, sugar metabolism, cell wall rearrangement, fruit aroma and lipid metabolism.

Mature fruit displayed more changes than ripe fruit, with several changes associated to well characterized pathways, in contrast to ripe fruit, where many changes could not be mapped to coordinated biochemical processes. This indicates that the metabolism of mature fruit is more regulated than the one from ripe fruit, which agrees with the idea that ripening fruit undergoes a coordinated senescence process.

Methods

Plant material

Large to medium-size fruit were harvested by trained professionals from the Institute of Agricultural Research (INIA), from 8-year-old 'O'Henry' trees grown on Nemaguard rootstocks in a commercial orchard located in the Aconcagua Valley, Chile (34o17' W, 70o54' S, Campos-Vargas et al., 2006). Change in fruit ground color measured using fruit company's color tables was considered as a harvesting index". Two postharvest stages were selected for proteome analysis: mature fruit (O1), that consisted on firm fruit taken immediately after harvest (firmness of around 60 N) and in the stage required for packing; and ripe fruit (O2), that consisted on fruit ripen at 20^{o}C (firmness of around 11 N, **Campos-Vargas et al., 2006**). Physiological parameters such as firmness, color, total soluble acids, titratable acidity, respiration rate and ethylene production were measured by Campos-Vargas et al. **(2006**). Three fruits from each postharvest stage were used for protein extraction and considered biological replicates (**Figure 1A**).

Protein extraction and SDS-PAGE

One milligram of mesocarp tissue from each biological sample was pulverized in liquid nitrogen and transferred to a room temperature tube with 5 mL of protein extraction buffer (**Abdi et al., 97**). This solution was mixed with 5.5 mL of Tris-saturated phenol pH 8.0 and shaken vigorously for 5 min at room temperature, followed by centrifugation at 8,500 × g for 14 min at 4°C to achieve aqueous/phenolic phase separation. The phenolic phase was recovered and re-extracted with an equal volume of protein extraction buffer. The resulting phenolic phase was precipitated for two hours at -20°C by the addition of five volumes of 0.1 M ammonium acetate in methanol at -20°C. The precipitated material was collected by centrifugation at 8,500 × g for 12 min and protein pellets were washed three times with cold ammonium acetate in methanol and once with 80% acetone at -20°C. The pellet was dried at room temperature and then solubilized in 300 µL of resuspension buffer which contained 5 M urea, 2 M thiourea, 2% CHAPS (w/v), 2% SB3-10 (w/v), 0.5% ampholites pH 5–7 (v/v) and 0.25% ampholites pH 3–10 (v/v) (**Mechin et al., 2003**). Protein yield was determined by Bradford protein assay (**Bradford MM., 1976**). All samples were stored at -80°C prior to electrophoresis.

SDS-PAGE was performed on 12% polyacrylamide gels casted on a BIO-RAD Mini-PROTEAN Tetra cell with 1 mm spacer plates. A hundred and fifty micrograms of protein samples were mixed with 10 µL

Coomassie blue 5X loading buffer and run at 80V until the dye front reached the bottom of the gel. Band visualization was achieved by staining the gels with colloidal Coomassie G250. Only one sample was run per gel. Each lane loaded with proteins was excised and divided into ten slices of 4 mm x 4mm x 1mm (**Figure 1B**).

Experimental LC/MS/MS

Gel slices were digested in-gel according to **Shevchenko et al. (1996)** with modifications. Gel bands were dehydrated using 100% acetonitrile and incubated with 10 mM dithiothreitol in 100 mM ammonium bicarbonate (pH 8) at 56ºC for 45 min, dehydrated again and incubated in the dark with 50 mM iodoacetamide in 100 mM ammonium bicarbonate for 20 min. Gel bands were then washed with ammonium bicarbonate and dehydrated again. Sequencing grade modified trypsin was prepared to a final concentration of 0.01mg mL^{-1} in 50 mM ammonium bicarbonate and 50 mL of this solution was added to each gel band. Bands were then incubated at 37ºC overnight. Peptides were extracted from the gel by water bath sonication in a solution of 60%ACN/1%TCA and vacuum dried to approximately 2 mL. Peptides were then re-suspended in 2% acetonitrile/0.1% trifluoroacetic acid to 20 mL. From this, 10 mL were automatically injected by a Waters nanoAcquity Sample Manager and loaded for 5 min onto a Waters Symmetry C18 peptide trap (5mm, 180mm x 20mm) at 4mL/min in 5%ACN/0.1% formic acid. The bound peptides were then loaded onto a Waters BEH C18 nanoAcquity column (1.7mm, 100mm x 100mm) and eluted for 35 min with a gradient of 5%B to 30%B in 24 min, ramped up to 90%B at 25 min and held for 1 min, then dropped back to 5%B at 26.1 min using a Waters nanoAcquity UPLC (Buffer A = 99.9% water/0.1% formic acid; Buffer B = 99.9% acetonitrile/0.1% formic acid) with a constant flow rate of 0.8mL min^{-1}.

Eluted peptides were sprayed into a ThermoFisher LTQ Linear Ion trap mass spectrometer outfitted with a MICHROM Bioresources ADVANCE nano-spray source. The top five ions in each survey scan were then subjected to data-dependent zoom scans followed by low energy collision induced dissociation (CID) and the resulting MS/MS spectra were converted to peak lists in BioWorks Browser v3.2 (www.thermo.com) using the default LTQ instrument parameters. Peak lists were searched against a custom database containing protein sequences from *Prunus persica* whole genome assembly, v1.0 and common laboratory contaminants (downloaded from NCBI, www.ncbi.nlm.nih.gov) using the Mascot searching algorithm, v2.3 (www.matrixscience.com). Mascot parameters for all databases were as follows: allow up to two missed tryptic sites; fixed modification of carbamidomethyl cysteine; variable modification of oxidation of methionine; peptide tolerance of +/- 200ppm; MS/MS tolerance of 0.6 Da; peptide charge state limited to +2/+3 (**Figure 1C**). Translation from v1.0 genome annotation to version 2.1 was achieved by using data provided by Phytozome v12 (**Goodstein et al., 2012**) and by manual analysis of the peptides characterized.

Data Processing

The Mascot output was analyzed using Scaffold v4.8.2 (www.proteomesoftware.com) to probabilistically validate protein identifications. Assignments were validated in Scaffold according to the following criteria: Protein Threshold - 1.0% FDR; Minimum number of peptides - 1; Peptide threshold - 0.1% FDR. To be able to accurately determine changes in protein levels, average total ion chromatograms (Average TIC) was retrieved from Scaffold for each protein assessed in each of the six samples under evaluation (**Asara et al., 2008**). Average TIC for each protein was estimated using only those peptides identified with high confidence (**Figure 1D**).

Data pre-treatment

To circumvent the issue of missing data, average values were calculated for those proteins that had only two biological replicates per biological condition (mature or ripe) and were used as third replicate. All the following analyses were thus performed with proteins which had at least two data points in O1 and O2, being the other proteins discarded. Protein data was scaled by using pareto scaling (**van den Berg et al., 2006**), normalized using Quantile Normalized procedure and centered at zero by subtracting the mean value, using InfernoRDN (version 1.1.5970.31895, **Taverner et al., 2012**). This allowed the data to be transformed to achieve a close to normal distribution, required for many statistical analyses of variance (**Supplementary Figure 1**). Q-Q and Box-plot graphs were also performed using InfernoRDN.

Assessment of the physicochemical characteristics of proteins

Proteins derived from the primary transcript of each of the 26,973 protein-coding genes (Ppersica_298_v2.1.protein_primaryTranscriptOnly.fa) were retrieved from Phytozome v12 (**Goodstein et al., 2012**) and were assessed using the Peptides R Package (**Osorio et al., 2015**). The following parameters were evaluated for each protein: length, molecular weight (MW, in Daltons), charge (pH = 7, pKscale = "Lehninger"), protein stability (instability index), and hydrophobicity (KyteDoolittle and Guy scale). Mean values and Gini's mean difference, a measure of variability that is robust even for non-normal data distributions, were computed using the Hmisc R Package.

Evaluation of protein differential accumulation

To detect differences in protein accumulation in mature and ripe fruits, a two-sample t-statistics with equal variance was performed for each protein/gene under analysis using the Bioconductor 'multtest' package followed by the "ABH" (Adaptive Benjamini-Hochberg) correction procedure, with a cutoff value of 0.1.

Gene ontology and pathways analysis

Gene ontology analysis was performed using Phytomine (https://phytozome.jgi.doe.gov/phytomine/begin.do). The Benjamini-Hochberg test, with a "max p-value" set to 0.05, was used for Multiple Testing Corrections. Redundant GO terms were removed with the webtool REVIGO (Supek et al., 2011), using the following parameters: 1. Allowed similarity: small (0.5); 2. GO categories associated to: p-values; 3. GO term sizes database: *Arabidopsis thaliana*; 4. Semantic

similarity measure to use: SimRel. Next, CirGO (**Kuznetsova et al., 2019**) was used to plot a concise version of the GO analysis.

Pathway diagrams were built by first running the program DeepEC (**Ryu et al., 2019**) to annotate the enzymes included in the 26,873 protein-coding genes from the *P. persica* genome version 2.1. Next, this annotation was used to generate the input file for the program Pathway Tools (**Karp et al., 2016**), which was used to infer the pathways and reactions from *P. persica* (**Supplementary File 1**).

Principal Component Analysis (PCA)

PCA analysis was run on normalized and centered data using the Explore/PCA tool from InfernoRDN (**Taverner et al., 2012**).

Transcriptional analysis of the Gene Expression Omnibus dataset GSE71561

Data from 13 peach samples, which included six samples from fruit seeds (days 41, 54, 69, 83, 111 and 125 after full bloom – DAFB), the same six samples from fruit mesocarp and one sample from flowers from the mid-season Fantasia variety, was downloaded from the GSE71561 dataset. Thus, samples covered until the commercial ripening stage.

The microarray data was log2 transformed following the protocol available from the online tool GEO2R (**Barrett et al., 2013**). This data, representing 29,045 genes, was used to generate heatmaps using the “superheat” R package (**Barter et al., 2018**). The main set parameters were: clustering.method = "hierarchical", dist.method = "maximum", linkage.method = "complete". In order to avoid dealing with probes that target the same gene, all genes were ranked according to their average abundance, and then those genes with repeated measures and lower average abundances were removed. Subsets of this data, such as expression patterns from selected protein-coding genes were also plotted as heatmaps using the same parameters.

In addition, data from mesocarp tissue was used to contrast the expression of genes in the 125 DAFB stage against the remaining five mesocarp samples (M_125 vs M_41, M_125 vs M_54, M_125 vs M_69, M_125 vs M_83, M_125 vs M_111). This task was performed using the Limma R package (**Ritchie et al., 2015**), following the protocol available from the online tool GEO2R (**Barrett et al., 2013**) and using the “decideTests” function. To improve the statistical confidence of the analysis, the probes that targeted the same gene had to display the same “decideTests” results in order to be considered for further analysis. This approach reduced the original dataset size from 29,045 genes to 18,074 genes (62.2%). These 18,074 genes included information from 1,136 protein-coding genes (68.3%) present in our proteomics dataset.

Retrieval and analysis of Transcription Factors regulatory elements

Transcription factors (TFs) that possessed over-represented targets in the protein set differentially accumulated in mature and ripe fruits and among all the proteins assessed in this study, were retrieved

from the Plant Transcription Factor Database (PlantTFDB, **Jin et al., 2017**), using the “Regulation Prediction” tool from the Plant Transcriptional Regulatory Map. Next, Phytomine (https://phytozome.jgi.doe.gov/phytomine/begin.do) was used to retrieve protein domains enriched for these TFs. The Benjamini-Hochberg test, with a “max p-value” set to 0.05, was used for Multiple Testing Corrections.

Gene family number analysis

P. persica gene family numbers were retrieved from PLAZA 4.0 (**Van Bel et al., 2018**), using the respective *P. persica* genome v2.1 ID as identifier.

Abbreviations

ACHT4 - atypical cysteine/histidine-rich thioredoxin 4

ACO - ACC oxidase

ACS - ACC synthase

APS1 - Glucose-1-phosphate adenylyltransferase small subunit

CXE - carboxylesterase

DAFB - days after full bloom

F6P - fructose 6-phosphate

FAD1 - Fatty acid desaturase 1

FERLs - Feronia-like receptor kinases

GO - Gene Ontology

PA - phosphatidic acid

PCA - Principal Component Analysis

PEP - phosphoenolpyruvate

PG - polygalacturonase

PLD - phospholipase D

SAM - S-Adenosyl methionine

SBE - 1,4-alpha-glucan-branching enzyme

SOT - sorbitol transporter

TFs - transcription factors

TIC - total ion chromatograms

Declarations

Affiliations

Escuela de Biotecnología, Facultad de Ciencias, Universidad Mayor, Camino La Pirámide 5750, Huechuraba, Chile.

Ricardo Nilo-Poyanco

Centro de Biotecnología Vegetal, Facultad Ciencias Biológicas, Universidad Andrés Bello, República 330, Santiago, Chile.

Gianfranco Benedetto & Ariel Orellana

Center for Genome Regulation, Blanco Encalada 2085, Santiago, Chile.

Ariel Orellana

Centro de Genómica y Bioinformática, Facultad de Ciencias, Universidad Mayor, Camino La Pirámide 5750, Huechuraba, Chile.

Escuela de Agronomía, Facultad de Ciencias, Universidad Mayor, Camino La Pirámide 5750, Huechuraba, Chile.

Andrea Miyasaka Almeida

Université Claude Bernard Lyon 1, 69622 Villeurbanne, France.

Inria Grenoble Rhône-Alpes, 38334 Montbonnot, France.

Carol Moraga

Declarations

Ethics approval and consent to participate

Not applicable.

Consent for publication

Not applicable.

Availability of data and material

Supporting material and protein datasets will be deposited at Springer Nature Research Data Support.

Competing interests

The authors declare that they have no competing interests.

Funding

The work was supported by Fondo Nacional de Desarrollo Científico y Tecnológico (Fondecyt, Chile) - Fondecyt Iniciación 11150107 to R.N-P. and Fondecyt Regular 1130197 to A.M.A.

Authors' Contributions

R.N-P. Protein extraction and display, bioinformatics and statistical analysis; C.M., G.B. collaborated on data analysis; A.O., A.M.A. experimental design, provided research opportunity; R.N-P., A.M.A. wrote the manuscript. All authors read and approved the final manuscript.

Acknowledgements

Doug Whitten from Research Technology Support Facility, Proteomics Core Facility at Michigan State University for advising in proteomics analysis. Dr Reinaldo Campos-Vargas for providing peach fruit mesocarp samples.

References

Abdallah C, Dumas-Gaudot E, Renaut J, Sergeant K. Gel-based and gel-free quantitative proteomics approaches at a glance. Int J Plant Genomics. 2012;2012:494572.

Abdi N, Holford P, Mcglasson B: Application of two-dimensional gel electrophoresis to detect proteins associated with harvest maturity in stonefruit. Postharvest Biol Tec 2002, 26 (1):1–13.

Aranzana MJ, Decroocq V, Dirlewanger E, et al. Prunus genetics and applications after de novo genome sequencing: achievements and prospects. Hortic Res. 2019;6:58.

Asara JM, Christofk HR, Freimark LM, Cantley LC. A label-free quantification method by MS/MS TIC compared to SILAC and spectral counting in a proteomics screen. Proteomics. 2008 Mar;8(5):994-9.

Barrett T, Wilhite SE, Ledoux P, et al. NCBI GEO: archive for functional genomics data sets–update. Nucleic Acids Res. 2013;41(Database issue):D991–D995.

Barter RL, Yu B. Superheat: An R package for creating beautiful and extendable heatmaps for visualizing complex data. J Comput Graph Stat. 2018;27(4):910–922.

Bianco L, Lopez L, Scalone AG, et al. Strawberry proteome characterization and its regulation during fruit ripening and in different genotypes. J Proteomics. 2009;72(4):586–607.

Bianchi VJ, Rubio M, Trainotti L, Verde I, Bonghi C, Martínez-Gómez P. Prunus transcription factors: breeding perspectives. Front Plant Sci. 2015 Jun 12;6:443.

Bradford MM. A rapid and sensitive method for the quantitation of microgram quantities of protein utilizing the principle of protein-dye binding. Anal Biochem 1976;72:248–54.

Campos-Vargas R, Becerra O, Baeza-Yates R, Cambiazo V, Gonzalez M, Meisel L, Orellana A, Retamales J, Silva H, Defilippi BG: Seasonal variation in the development of chilling injury in 'O'Henry' peaches. Sci Hortic-Amsterdam 2006, 110 (1):79–83.

Cai H, Han S, Jiang L, Yu M, Ma R, Yu Z. 1-MCP treatment affects peach fruit aroma metabolism as revealed by transcriptomics and metabolite analyses. Food Res Int. 2019 Aug;122:573-584.

Cantín, C.M., Gogorcena, Y. and Moreno, M.Á., 2009. Analysis of phenotypic variation of sugar profile in different peach and nectarine [Prunus persica (L.) Batsch] breeding progenies. Journal of the Science of Food and Agriculture, 89(11), pp.1909-1917.

Cao K, Zheng Z, Wang L, Liu X, Zhu G, Fang W, Cheng S, Zeng P, Chen C, Wang X, Xie M, Zhong X, Wang X, Zhao P, Bian C, Zhu Y, Zhang J, Ma G, Chen C, Li Y, Hao F, Li Y, Huang G, Li Y, Li H, Guo J, Xu X, Wang J. Comparative population genomics reveals the domestication history of the peach, Prunus persica, and human influences on perennial fruit crops. Genome Biol. 2014 Jul 31;15(7):415.

Cao S, Liang M, Shi L, Shao J, Song C, Bian K, Chen W, Yang Z. Accumulation of carotenoids and expression of carotenogenic genes in peach fruit. Food Chem. 2017a Jan 1;214:137-146.

Cao K, Ding T, Mao D, Zhu G, Fang W, Chen C, Wang X, Wang L. Transcriptome analysis reveals novel genes involved in anthocyanin biosynthesis in the flesh of peach. Plant Physiol Biochem. 2017b Dec 7;123:94-102.

Cao X, Xie K, Duan W, et al. Peach Carboxylesterase PpCXE1 Is Associated with Catabolism of Volatile Esters. J Agric Food Chem. 2019;67(18):5189–5196.

Chen YH, Khanal BP, Linde M, Debener T, Alkio M, Knoche M. Expression of putative aquaporin genes in sweet cherry is higher in flesh than skin and most are downregulated during development. Scientia horticulturae. 2019 Jan 26;244:304-14.

Cirilli M, Bassi D, Ciacciulli A. Sugars in peach fruit: a breeding perspective. Hortic Res. 2016;3:15067. Published 2016 Jan 20.

D'Ambrosio C, Arena S, Rocco M, Verrillo F, Novi G, Viscosi V, Marra M, Scaloni A. Proteomic analysis of apricot fruit during ripening. J Proteomics. 2013 Jan 14;78:39-57.

Desnoues E, Génard M, Quilot-Turion B, Baldazzi V. A kinetic model of sugar metabolism in peach fruit reveals a functional hypothesis of a markedly low fructose-to-glucose ratio phenotype. Plant J. 2018;94(4):685–698.

Eliyahu E, Rog I, Inbal D, Danon A. ACHT4-driven oxidation of APS1 attenuates starch synthesis under low light intensity in Arabidopsis plants. Proc Natl Acad Sci U S A. 2015;112(41):12876–12881.

Etienne A, Génard M, Lobit P, Mbeguié-A-Mbéguié D, Bugaud C. What controls fleshy fruit acidity? A review of malate and citrate accumulation in fruit cells. J Exp Bot. 2013 Apr;64(6):1451-69.

Famiani F, Farinelli D, Moscatello S, Battistelli A, Leegood RC, Walker RP. The contribution of stored malate and citrate to the substrate requirements of metabolism of ripening peach (Prunus persica L. Batsch) flesh is negligible. Implications for the occurrence of phosphoenolpyruvate carboxykinase and gluconeogenesis. Plant Physiol Biochem. 2016 Apr;101:33-42.

Fang Y, Robinson DP, Foster LJ. Quantitative analysis of proteome coverage and recovery rates for upstream fractionation methods in proteomics. J Proteome Res. 2010 Apr 5;9(4):1902-12.

Gapper NE, McQuinn RP, Giovannoni JJ. Molecular and genetic regulation of fruit ripening. Plant Mol Biol. 2013 Aug;82(6):575-91.

Gapper NE, Giovannoni JJ, Watkins CB. Understanding development and ripening of fruit crops in an 'omics' era. Hortic Res. 2014 Jul 23;1:14034.

Fan RC, Peng CC, Xu YH, et al. Apple sucrose transporter SUT1 and sorbitol transporter SOT6 interact with cytochrome b5 to regulate their affinity for substrate sugars. Plant Physiol. 2009;150(4):1880–1901.

Gao Z, Maurousset L, Lemoine R, Yoo SD, van Nocker S, Loescher W. Cloning, expression, and characterization of sorbitol transporters from developing sour cherry fruit and leaf sink tissues. Plant Physiol. 2003;131(4):1566–1575.

Goodstein DM, Shu S, Howson R, Neupane R, Hayes RD, Fazo J, Mitros T, Dirks W, Hellsten U, Putnam N, Rokhsar DS. Phytozome: a comparative platform for green plant genomics. Nucleic Acids Res. 2012 Jan;40(Database issue):D1178-86.

Hayama H, Shimada T, Fujii H, Ito A, Kashimura Y. Ethylene-regulation of fruit softening and softening-related genes in peach. J Exp Bot. 2006;57(15):4071–4077.

Jiang L, Feng L, Zhang F, Luo H, Yu Z. Peach fruit ripening: Proteomic comparative analyses of two cultivars with different flesh texture phenotypes at two ripening stages. Scientia Horticulturae. 2020 Jan 27;260:108610.

Jincy M, Djanaguiraman M, Jeyakumar P, Subramanian KS, Jayasankar S, Paliyath G. Inhibition of phospholipase D enzyme activity through hexanal leads to delayed mango (Mangifera indica L.) fruit ripening through changes in oxidants and antioxidant enzymes activity. Scientia Horticulturae. 2017 Apr 14;218:316-25.

Karp PD, Latendresse M, Paley SM, et al. Pathway Tools version 19.0 update: software for pathway/genome informatics and systems biology. Brief Bioinform. 2016;17(5):877–890.

Guizani, M., Maatallah, S., Dabbou, S., Serrano, M., Hajlaoui, H., Helal, A.N. and Kilani-Jaziri, S., 2019. Physiological behaviors and fruit quality changes in five peach cultivars during three ripening stages in a semi-arid climate. Acta Physiologiae Plantarum, 41(9), p.154.

Guy HR. Amino acid scale: Hydrophobicity scale based on free energy of transfer (kcal/mole). Biophys J. 1985;47:61-70.

Kuznetsova I, Lugmayr A, Siira SJ, Rackham O, Filipovska A. CirGO: an alternative circular way of visualising gene ontology terms. BMC Bioinformatics. 2019;20(1):84.

Jia M, Du P, Ding N, et al. Two FERONIA-Like Receptor Kinases Regulate Apple Fruit Ripening by Modulating Ethylene Production. Front Plant Sci. 2017;8:1406. Published 2017 Aug 10. doi:10.3389/fpls.2017.01406

Jin J, Tian F, Yang DC, Meng YQ, Kong L, Luo J, Gao G. PlantTFDB 4.0: toward a central hub for transcription factors and regulatory interactions in plants. Nucleic Acids Res. 2017 Jan 4;45(D1):D1040-D1045.

Li XW, Jiang J, Zhang LP, Yu Y, Ye ZW, Wang XM, Zhou JY, Chai ML, Zhang HQ, Arús P, Jia HJ. Identification of volatile and softening-related genes using digital gene expression profiles in melting peach. Tree genetics & genomes. 2015 Aug 1;11(4):71.

Lindemann C, Thomanek N, Hundt F, Lerari T, Meyer HE, Wolters D, Marcus K. Strategies in relative and absolute quantitative mass spectrometry based proteomics. Biol Chem. 2017 May 1;398(5-6):687-699.

Lü P, Yu S, Zhu N, Chen YR, Zhou B, Pan Y, Tzeng D, Fabi JP, Argyris J, Garcia-Mas J, Ye N, Zhang J, Grierson D, Xiang J, Fei Z, Giovannoni J, Zhong S. Genome encode analyses reveal the basis of convergent evolution of fleshy fruit ripening. Nat Plants. 2018 Oct;4(10):784-791.

Molloy MP, Herbert BR, Williams KL, Gooley AA. Extraction of Escherichia coli proteins with organic solvents prior to two-dimensional electrophoresis. Electrophoresis. 1999;20(4-5):701–704.

Monti LL, Bustamante CA, Osorio S, Gabilondo J, Borsani J, Lauxmann MA, Maulión E, Valentini G, Budde CO, Fernie AR, Lara MV, Drincovich MF. Metabolic profiling of a range of peach fruit varieties reveals high metabolic diversity and commonalities and differences during ripening. Food Chem. 2016 Jan 1;190:879-88.

Monti LL, Bustamante CA, Budde CO, Gabilondo J, Müller GL, Lara MV, Drincovich MF. Metabolomic and proteomic profiling of Spring Lady peach fruit with contrasting woolliness phenotype reveals carbon oxidative processes and proteome reconfiguration in chilling-injured fruit. Postharvest Biology and Technology. 2019 May 1;151:142-51.

Nilo-Poyanco R, Saffie C, Lilley K, Baeza-Yates R, Cambiazo V, Campos-Vargas R, González M, Meisel LA, Retamales J, Silva H, Orellana A. Proteomic analysis of peach fruit mesocarp softening and chilling injury using difference gel electrophoresis (DIGE). BMC Genomics. 2010 Jan 18;11:43.

Nilo-Poyanco R, Campos-Vargas R, Orellana A. Assessment of Prunus persica fruit softening using a proteomics approach. J Proteomics. 2012 Feb 16;75(5):1618-38.

Nilo-Poyanco R, Vizoso P, Sanhueza D, et al. A Prunus persica genome-wide RNA-seq approach uncovers major differences in the transcriptome among chilling injury sensitive and non-sensitive varieties. Physiol Plant. 2019;166(3):772–793.

Nuñez, C., Dupré, G., Mujica, K. et al. Thinning alters the expression of the PpeSUT1 and PpeSUT4 sugar transporter genes and the accumulation of translocated sugars in the fruits of an early season peach variety. Plant Growth Regul 88, 283–296 (2019).

Osorio D, Rondón-Villarrea P. and Torres R, 2015. Peptides: a package for data mining of antimicrobial peptides. R Journal, 7(1).

Pegoraro C, Tadiello A, Girardi CL, Chaves FC, Quecini V, de Oliveira AC, Trainotti L, Rombaldi CV. Transcriptional regulatory networks controlling woolliness in peach in response to preharvest gibberellin

application and cold storage. BMC Plant Biol. 2015 Nov 18;15:279.

Pirona R, Vecchietti A, Lazzari B, et al. Expression profiling of genes involved in the formation of aroma in two peach genotypes. Plant Biol (Stuttg). 2013;15(3):443–451.

Qian M, Zhang Y, Yan X, et al. Identification and Expression Analysis of Polygalacturonase Family Members during Peach Fruit Softening. Int J Mol Sci. 2016;17(11):1933.

Qin C, Wang C, Wang X. Kinetic analysis of Arabidopsis phospholipase Ddelta. Substrate preference and mechanism of activation by Ca2+ and phosphatidylinositol 4,5-biphosphate. J Biol Chem. 2002;277(51):49685–49690.

Regon P, Panda P, Kshetrimayum E, Panda SK. Genome-wide comparative analysis of tonoplast intrinsic protein (TIP) genes in plants. *Funct Integr Genomics*. 2014;14(4):617–629.

Ren H, Willige BC, Jaillais Y, et al. BRASSINOSTEROID-SIGNALING KINASE 3, a plasma membrane-associated scaffold protein involved in early brassinosteroid signaling. *PLoS Genet*. 2019;15(1):e1007904.

Ritchie ME, Phipson B, Wu D, et al. limma powers differential expression analyses for RNA-sequencing and microarray studies. Nucleic Acids Res. 2015;43(7):e47.

Ruperti B, Bonghi C, Rasori A, Ramina A, Tonutti P. Characterization and expression of two members of the peach 1-aminocyclopropane-1-carboxylate oxidase gene family. Physiol Plant. 2001;111(3):336–344.

Ryu JY, Kim HU, Lee SY. Deep learning enables high-quality and high-throughput prediction of enzyme commission numbers. Proc Natl Acad Sci U S A. 2019;116(28):13996–14001.

Sánchez G, Venegas-Calerón M, Salas JJ, Monforte A, Badenes ML, Granell A. An integrative "omics" approach identifies new candidate genes to impact aroma volatiles in peach fruit. BMC Genomics. 2013 May 23;14:343.

Sánchez-Sevilla JF, Cruz-Rus E, Valpuesta V, Botella MA, Amaya I. Deciphering gamma-decalactone biosynthesis in strawberry fruit using a combination of genetic mapping, RNA-Seq and eQTL analyses. *BMC Genomics*. 2014;15:218.

Shevchenko, A., Wilm, M., Vorm, O., Mann, M. Anal Chem. 1996 Mar 1;68(5):850-8.

Tadiello A, Ziosi V, Negri AS, Noferini M, Fiori G, Busatto N, Espen L, Costa G, Trainotti L. On the role of ethylene, auxin and a GOLVEN-like peptide hormone in the regulation of peach ripening. BMC Plant Biol. 2016 Feb 11;16:44.

Taverner T, Karpievitch YV, Polpitiya AD, Brown JN, Dabney AR, Anderson GA, Smith RD. DanteR: an extensible R-based tool for quantitative analysis of -omics data. Bioinformatics. 2012 Sep

15;28(18):2404-6.

Trainotti L, Spolaore S, Ferrarese L, Casadoro G. Characterization of ppEG1, a member of a multigene family which encodes endo-beta-1,4-glucanase in peach. Plant Mol Biol. 1997;34(5):791–802.

Trainotti L, Zanin D, Casadoro G. A cell wall-oriented genomic approach reveals a new and unexpected complexity of the softening in peaches. J Exp Bot. 2003 Aug;54(389):1821-32.

Van Bel M, Diels T, Vancaester E, et al. PLAZA 4.0: an integrative resource for functional, evolutionary and comparative plant genomics. Nucleic Acids Res. 2018;46(D1):D1190–D1196.

van den Berg RA, Hoefsloot HC, Westerhuis JA, Smilde AK, van der Werf MJ. Centering, scaling, and transformations: improving the biological information content of metabolomics data. BMC Genomics. 2006 Jun 8;7:142.

Velasco D, Hough J, Aradhya M, Ross-Ibarra J. Evolutionary Genomics of Peach and Almond Domestication. G3 (Bethesda). 2016;6(12):3985–3993.

Verde I, Jenkins J, Dondini L, Micali S, Pagliarani G, Vendramin E, Paris R, Aramini V, Gazza L, Rossini L, Bassi D, Troggio M, Shu S, Grimwood J, Tartarini S, Dettori MT, Schmutz J. The Peach v2.0 release: high-resolution linkage mapping and deep resequencing improve chromosome-scale assembly and contiguity. BMC Genomics. 2017 Mar 11;18(1):225.

Vimolmangkang S, Zheng H, Peng Q, Jiang Q, Wang H, Fang T, Liao L, Wang L, He H, Han Y. Assessment of Sugar Components and Genes Involved in the Regulation of Sucrose Accumulation in Peach Fruit. J Agric Food Chem. 2016 Sep 7;64(35):6723-9.

Wang JJ, Liu HR, Gao J, Huang YJ, Zhang B, Chen KS. Two ω-3 FADs Are Associated with Peach Fruit Volatile Formation. Int J Mol Sci. 2016 Mar 29;17(4):464.

Wang X, Ding Y, Wang Y, Pan L, Niu L, Lu Z, Cui G, Zeng W, Wang Z. Genes involved in ethylene signal transduction in peach (*Prunus persica*) and their expression profiles during fruit maturation. Scientia Horticulturae. 2017, 224:306-316.

Wang X, Zeng W, Ding Y, et al. Peach ethylene response factor PpeERF2 represses the expression of ABA biosynthesis and cell wall degradation genes during fruit ripening. *Plant Sci*. 2019;283:116–126.

Wei X, Liu F, Chen C, Ma F, Li M. The Malus domestica sugar transporter gene family: identifications based on genome and expression profiling related to the accumulation of fruit sugars. Front Plant Sci. 2014;5:569.

Yu CY, Cheng HY, Cheng R, Qi KJ, Gu C, Zhang SL. Expression analysis of sorbitol transporters in pear tissues reveals that PbSOT6/20 is associated with sorbitol accumulation in pear fruits. Scientia horticulturae. 2019 Jan 3;243:595-601.

Zhang B, Shen JY, Wei WW, et al. Expression of genes associated with aroma formation derived from the fatty acid pathway during peach fruit ripening. J Agric Food Chem. 2010;58(10):6157–6165.

Zhang L, Li H, Gao L, Qi Y, Fu W, Li X, Zhou X, Gao Q, Gao Z, Jia H. Acyl-CoA oxidase 1 is involved in γ-decalactone release from peach (*Prunus persica*) fruit. Plant Cell Rep. 2017 Jun;36(6):829-842.

Zhao Q, Liu C. Chloroplast Chaperonin: An Intricate Protein Folding Machine for Photosynthesis. Front Mol Biosci. 2018;4:98.

Zhu, Y., Zeng, W., Wang, X., Pan, L., Niu, L., Lu, Z., Cui, G. and Wang, Z., 2017. Characterization and Transcript Profiling of PME and PMEI Gene Families during Peach Fruit Maturation. Journal of the American Society for Horticultural Science, 142(4), pp.246-259.

Supplementary Information

Supplementary Figure 1. Data pre-treatment. In order to have an insight about the data distribution, Q-Q plots were generated using as input the raw (**A**), versus imputed-scaled-centered protein abundance data (**C**). As a result from pre-treatment data, the Q-Q plot curve fitted much closer to the normal expectation curve (straight red diagonal line) than with the raw data. Boxplots of raw (**B**) vs treated data (**D**) further highlighted how the data became centered and scaled after been pre-treated.

Supplementary Figure 2. Proteome bias assessment. Protein parameters were compared among *P. persica* primary transcripts' proteome (left panels), current proteome (middle panels) and a mesocarp-derived proteome extracted from juicy and mealy fruits from the Spring Lady variety (right panels, Monti et al. 2019). Panels I to III contrast proteomes in terms of length and molecular weights (MW). Panels IV to VI contrast proteomes in terms of charge and protein stability based on its amino acids (instalindex). Panels VII to IX contrast proteomes in terms of hydrophobicity, using two scales: KyteDoolittle and Guy. Each dot in each graph represents the intersection of the values one protein has for the two parameters under evaluation. The distributions of values for each of these two parameters are shown above and at the right side of each panel as density plots.

Supplementary Figure 3. Hierarchical clustering of all genes transcriptionally characterized in the GSE71561 dataset and a subset related to sorbitol biosynthesis. Transcriptional information (average of three replicates of log2 normalized fluorescence intensity values) from 29,045 genes from the peach fruit genome 1.0, assessed in 13 conditions, was displayed using hierarchical clustering and the following conditions: clustering.method = "hierarchical", dist.method = "maximum", linkage.method = "complete" (**panel I**). Using the same stages, data from genes encoding a putative sorbitol transporter family is also depicted (panel II). S_45 to S_125, seed samples at 45, 54, 69, 83, 111 and 125 days after full bloom (DAFB); M_45 to M_125, mesocarp samples at 45, 54, 69, 83, 111 and 125 DAFB; F - flower samples.

Supplementary Figure 4. Comparison of the O'Henry fruit mesocarp proteome characterized by 2D gel vs 1D gel analysis. **(a)** Mesocarp proteins from mature and ripe O'Henry fruits assessed by 2D-gels had 164

spots that could be quantified (Nilo-Poyanco et al., 2012). Among these 164 spots, 43 were identified by mass spectrometry analysis and, therefore, were contrasted with the current proteome under analysis. **(b)** Among these 43 proteins, 16 had accumulation profiles similar to the ones assessed in the current work ("match"), whereas 27 had different patterns ("did not match").

Table

Due to technical limitations, table 1 is only available as a download in the supplemental files section.

Figures

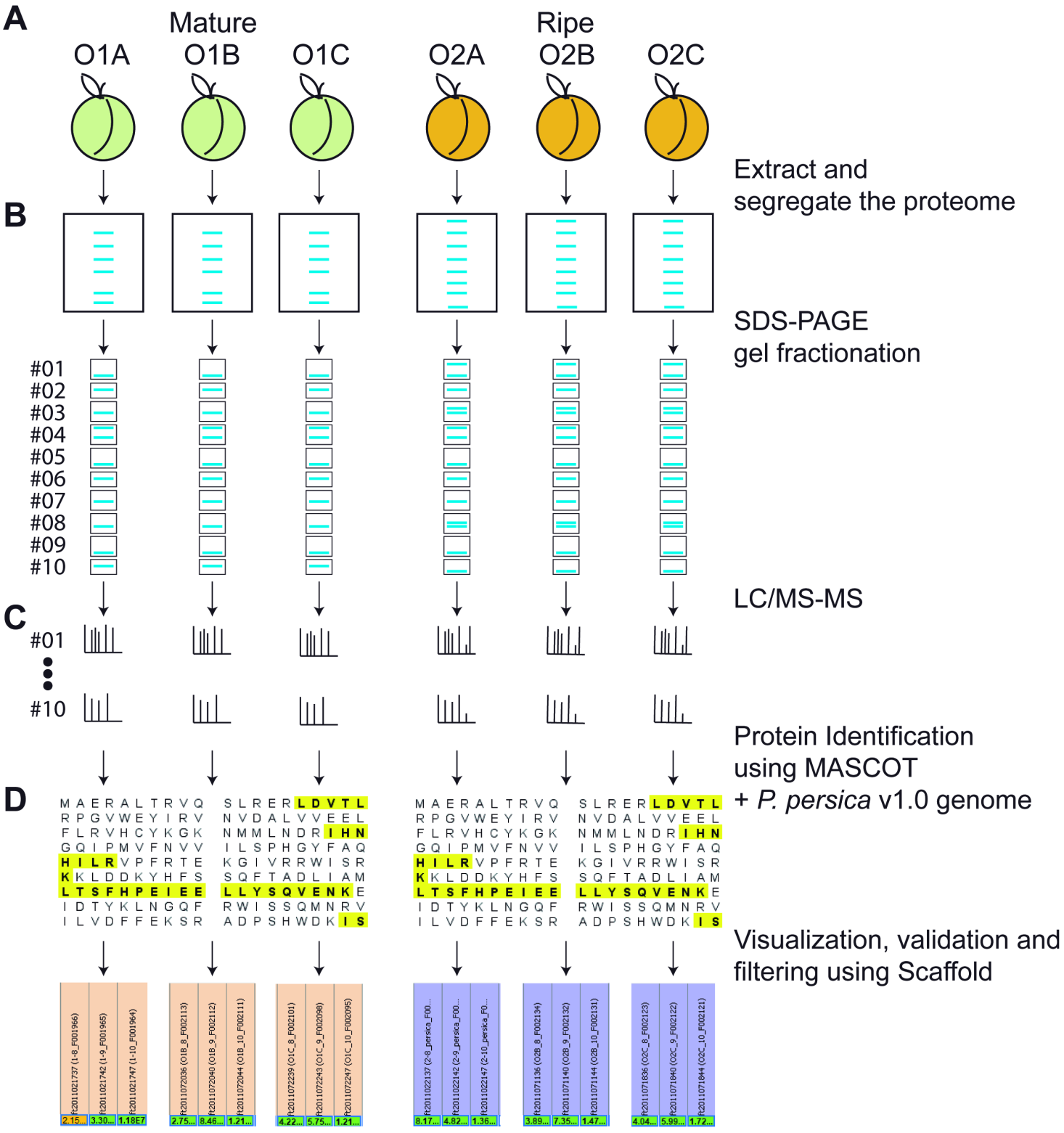

Figure 1

Proteomics shotgun approach used to uncover proteins involved in peach fruit mesocarp ripening process. (a) Mesocarp proteins were extracted from three biological samples (OH1A-C, OH2A-C) of mature and ripe 'O'Henry' peach fruit. (b) Proteins were separated using SDS-PAGE gels and later fractioned in 10 gel slices. (c) The proteins present in each slice were sequenced through LC/MS-MS. (d) The identity of the peptides present in each gel slice was assessed using Mascot and the genome

sequence from Prunus persica v1.0. Identified proteins were further assessed using Scaffold (version 4.8.2) to identify those proteins associated with highly confident peptides and to export appropriate data for subsequent quantitative analysis (see Methods section).

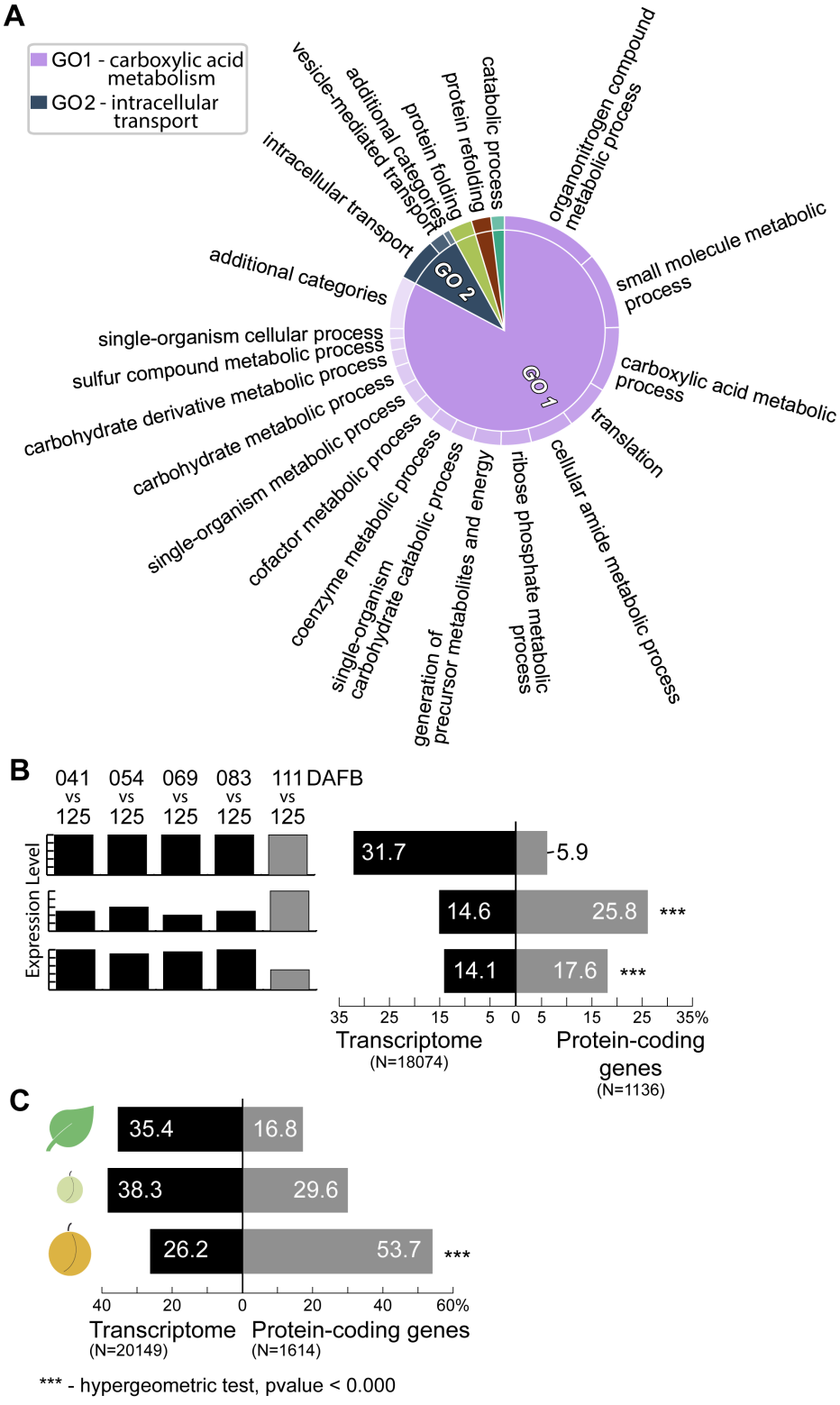

Figure 2

Analysis of global patterns in the proteomics dataset and comparison with related transcriptomic data. (a) Gene Ontology analysis of the 1,163 proteins assessed indicated that this set was enriched in

carboxylic acid metabolism, intracellular transport, and to a lesser extent in protein folding. (b) Expression levels from 18,074 genes from the “Fantasia” variety were assessed at 41, 54, 69, 83, 111 and 125 (ripe fruit) days after full bloom (DAFB). The analysis indicated that 31.7% of the genes did not display any change when comparing each developmental stage against ripe fruit, 14.6% displayed its highest level and 14.1% its lowest level at ripe fruit stage (black bars, first, second and third lane, respectively). When assessing the protein-coding genes detected in mature + ripe fruit (present study), it was estimated that 5.9% did not display any change when comparing each developmental stage against ripe fruit, 25.8% displayed its highest level and 17.6% displayed its lowest level at ripe fruit stage (grey bars, first, second and third lane, respectively). The last two analyses in ripe fruit yielded statistically significant results. (c) Expression levels from 20,149 genes of the “Babygold” variety were assessed in leaves, immature and ripe fruit. Genes that were more expressed in leaves compared to immature and ripe fruit tissues using the full transcriptome dataset accounted for 35.4% of the genes (black bars). This number dropped to 16.8% when using the proteomics dataset (grey bars). The same kind of comparison performed on the genes that were more expressed in the immature and ripe fruit yielded percentages of 38.3% vs 29.6% and 26.2% vs 53.7%, being the difference found in ripe fruit statistically significant.

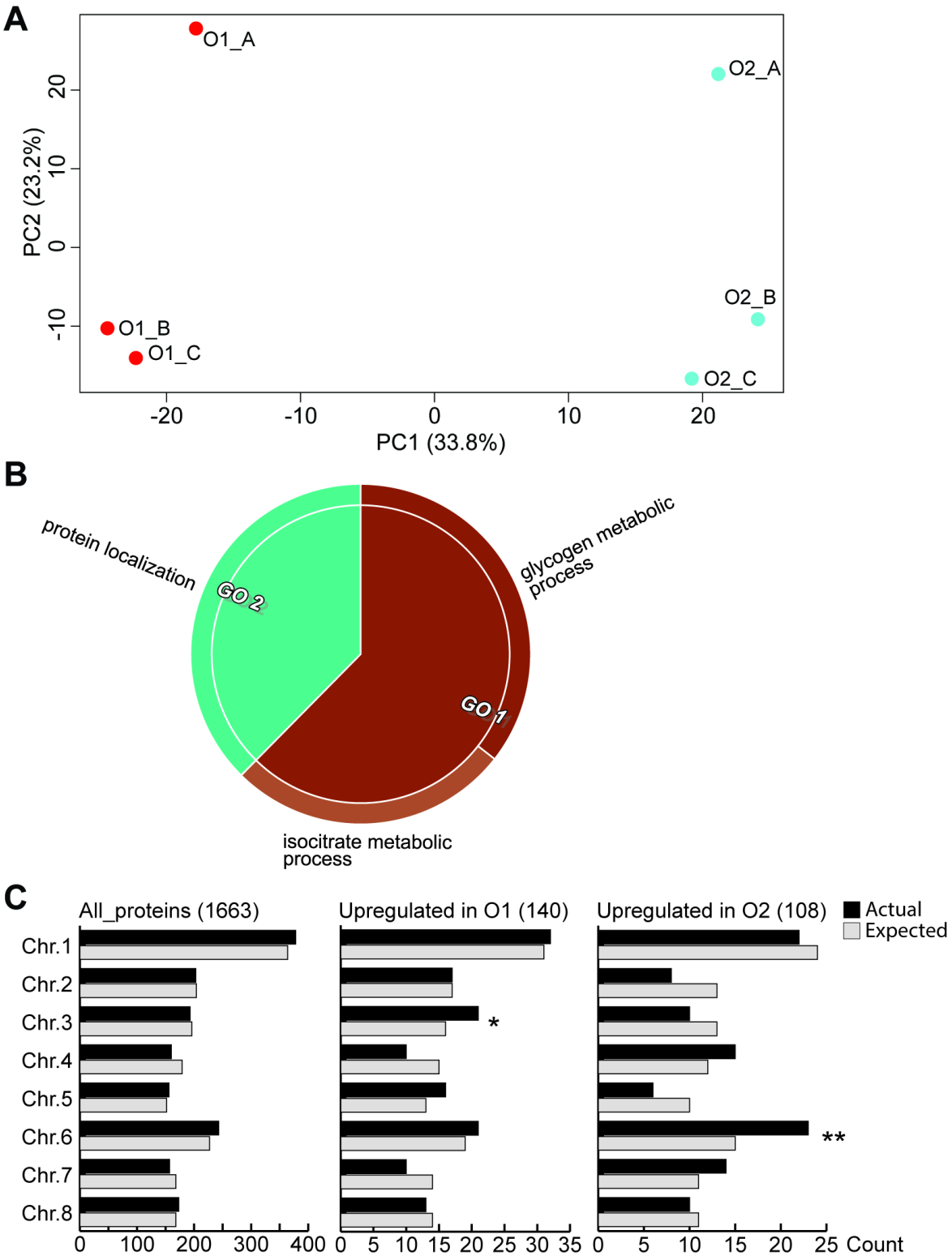

Figure 3

Analysis of proteins differentially accumulated in mature and ripe fruit. (a) All 1,663 proteins detected in mature (O1) and ripe (O2) fruit were used to perform a Principal Component Analysis (PCA), with PC1 segregating mature from ripe fruit (A). From these 1,663 proteins, 248 displayed a differential accumulation in O1 and O2 samples. (b) The main biological processes related to the differentially accumulated proteins in O1 fruit were associated to glycogen and isocitrate metabolism, and protein

localization. (c) When assessing all the 1,663 characterized proteins (“All_proteins”), no enrichment was found. Among the proteins upregulated in mature fruit, those with protein-coding genes in chromosome 3 (actual, black bars) were more than expected by chance (expected, grey bars, hypergeometric test, pvalue < 0.05). The same analysis determined that those protein-coding genes upregulated in ripe fruit were located, more than expected by chance, in chromosome 6 (pvalue < 0.01). Chr. - Chromosome.

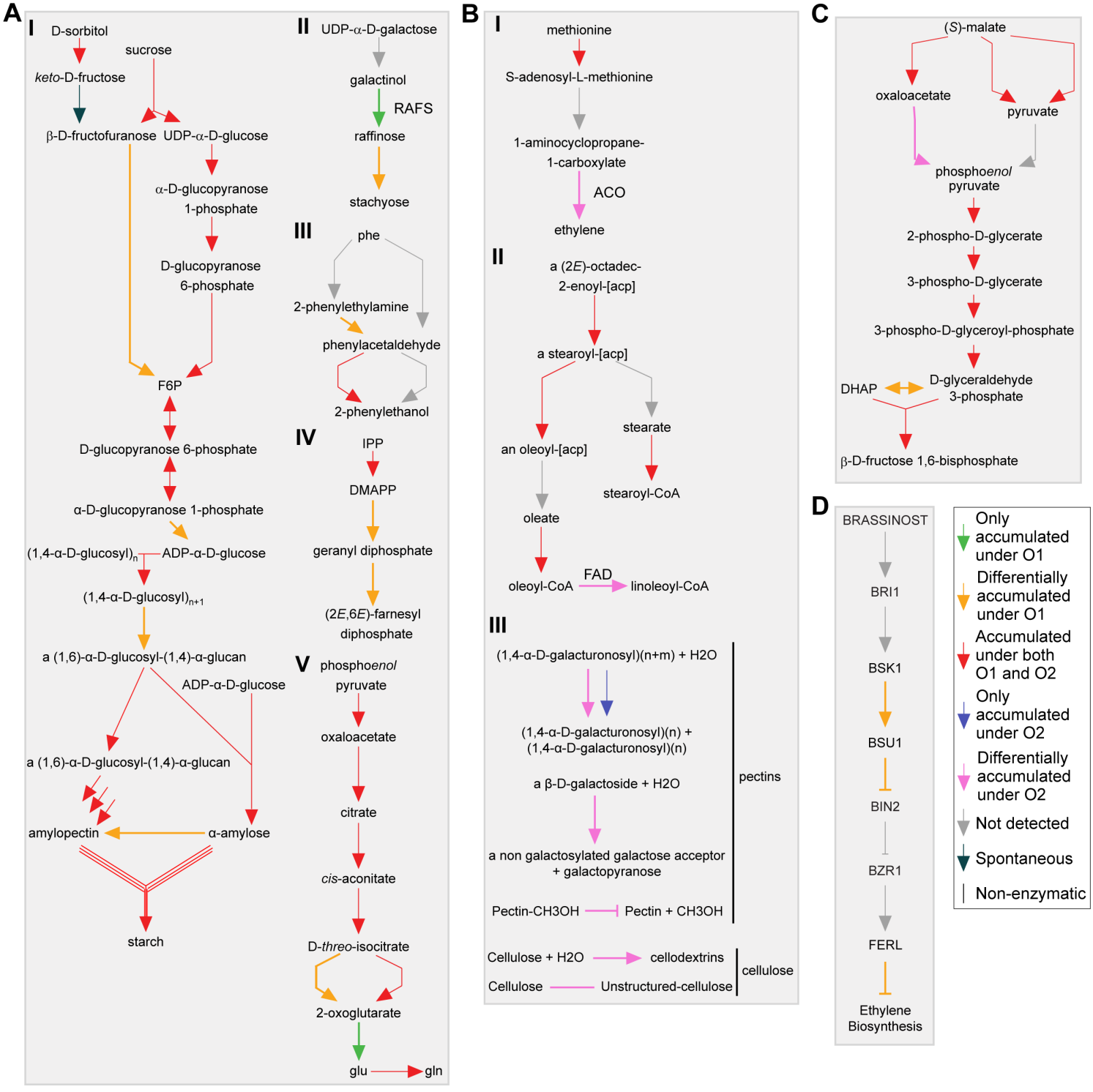

Figure 4

Analysis of biological processes and pathways associated to differentially accumulated proteins. (a) Sucrose and sorbitol conversion into fructose 6-phosphate (F6P), and thereafter into starch, would preferentially occur at the mature fruit stage (panel I, MetaCyc pathways PWY-3801 and PWY-622). Raffinose and stachyose (PWY-5337), phenylacetaldehyde (PWY-5751), farnesyl diphosphate (PWY-5123) and glutamine (PWY-6549) biosynthetic pathways also had proteins that were more abundant in mature fruit (panels II to V). (b) In turn, ethylene (ETHYL-PWY) and linoleoyl-CoA (PWY-6001) would be preferentially synthesized in ripe fruit due to the preferential accumulation of enzymes related to these pathways at this stage (panels I and II). Cell-wall dismantling would also be favored when the fruit ripens due to the accumulation of pectin and cellulose modifying proteins and enzymes (panel III). (c) Gluconeogenesis (GLUCONEO-PWY) related enzymes were found accumulated in mature and ripe fruit, but with differences at the glycerone phosphate - D-glyceraldehyde 3-phosphate interconversion step (O1, EC 5.3.1.1) and the oxaloacetate conversion into phosphoenolpyruvate (O2, EC 4.1.1.49), which had differentially accumulated proteins associated to mature and ripe fruit. (d) Ethylene biosynthesis in mature fruit would be negatively modulated by the action of the signaling cascade that would begin with the action of brassinosteroids and culminate with Feronia-like receptor kinases (FERLs) action upon genes involved in ethylene biosynthesis. F-6-P - fructose 6-phosphate; RAFS - raffinose synthase; phe - phenylalanine; IPP - isopentenyl diphosphate; DMAPP - prenyl diphosphate; glu - glutamate; gln - glutamine; ACO - 1-aminocyclopropane-1-carboxylate oxidase; FAD - Fatty acid desaturase.

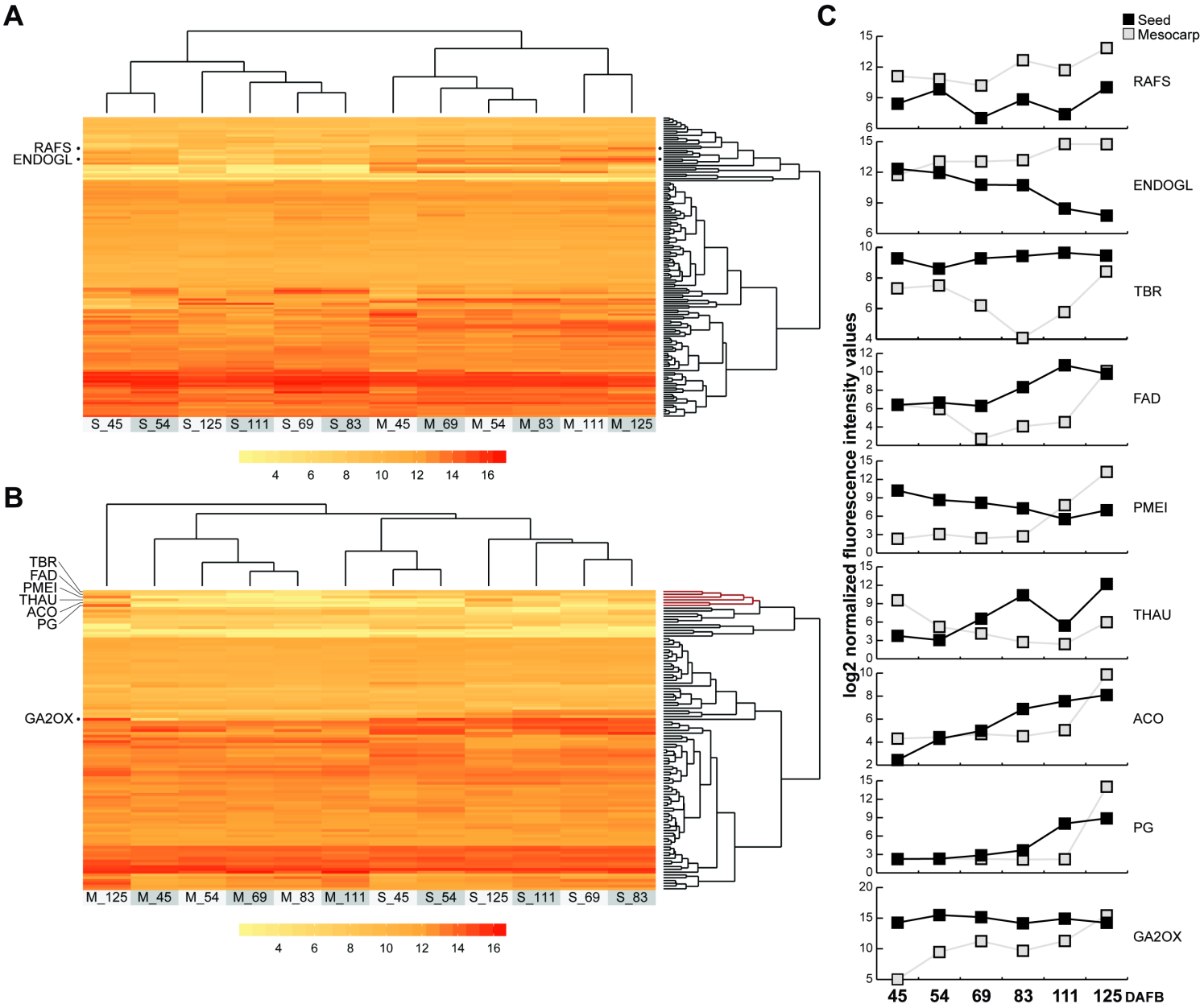

Figure 5

Transcriptome analysis of protein-coding genes assessed in this work throughout the fruit development curve. (a) Gene expression data (GEO GSE71561) from the genes that code for the 248 differentially accumulated proteins assessed in this work, was retrieved from the Fantasy variety for six developmental stages and two tissues, seeds and mesocarp. Hierarchical cluster analysis revealed that, when considering the 140 genes from differentially accumulated proteins in mature fruit mesocarp, stages 111 and 125 DAFB (M_111, M_125) were set apart from all other conditions. (b) This pattern changed when considering proteins that were differentially accumulated in ripe fruit, with stage M_125 being set apart from any other cluster. (c) Expression patterns of the genes that showed their highest expression at M_125, highlighted at the left side of the hierarchical clusters shown in (a) and (b), is depicted. Several of these genes were concentrated in the same cluster (highlighted in red in the upper segment of the figure (b)). RAFS - raffinose synthase, Prupe.6G032400; ENDOGL - endoglucanase - Prupe.5G118000; TBR -

Protein Trichome Birefringence-like 41, Prupe.4G157600; FAD - Fatty acid desaturase - Prupe.7G076500; PMEI - Plant invertase/pectin methylesterase inhibitor, Prupe.1G114500; THAU - thaumatin, Prupe.3G144100; ACO - 1-aminocyclopropane-1-carboxylate oxidase, Prupe.3G209900; PG - polygalacturonase, Prupe.4G262200; GA2OX - Gibbellerin 2-beta-dioxygenase 4, Prupe.1G111900.

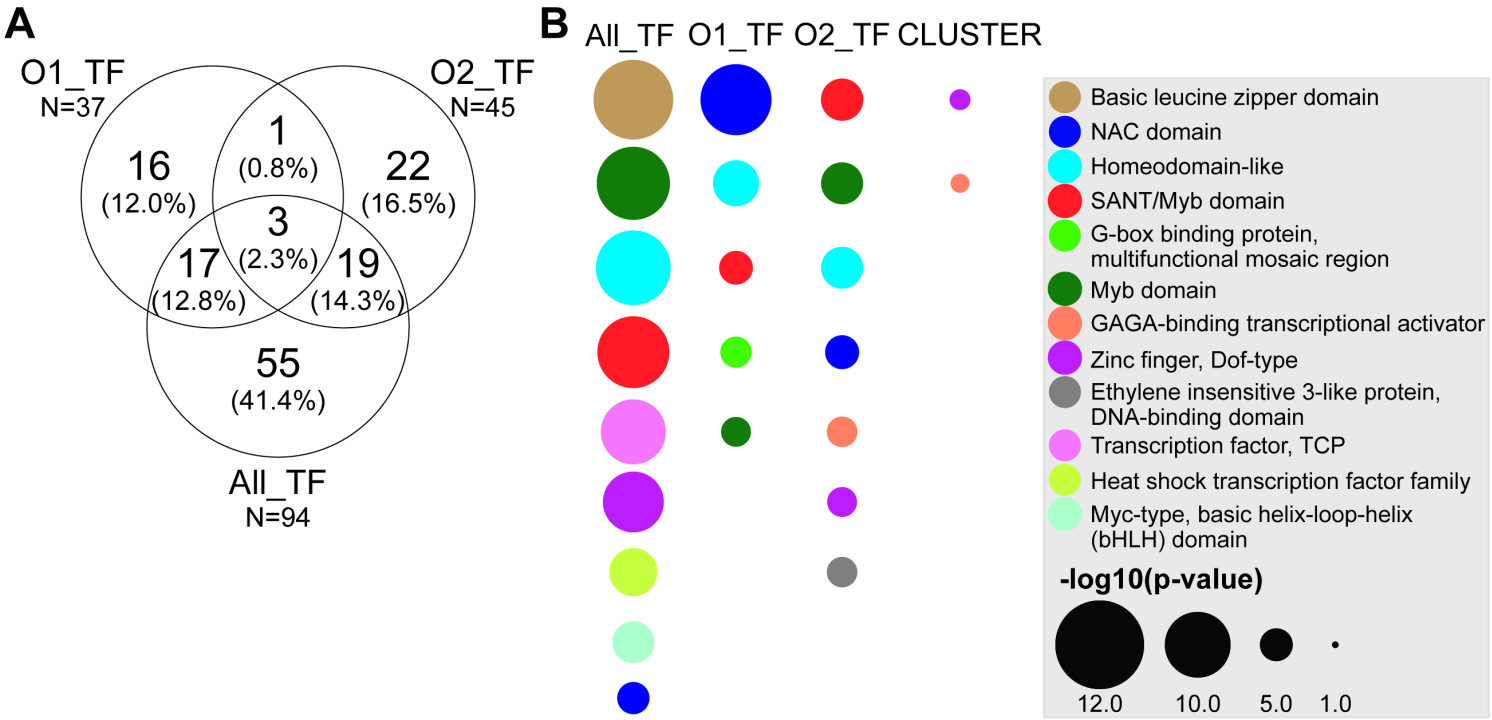

Figure 6

Analysis of transcription factors with over-represented targets in the set of differentially accumulated proteins. (a) Ninety-four, thirty-seven and forty-five transcription factors (TFs) were found to have over-represented targets among the proteins assessed in this study (“ALL_TF”), those differentially accumulated in mature fruit (“O1_TF”), and those differentially accumulated in ripe fruit (“O2_TF”). (b) An analysis of TF protein domains indicated that “ALL_TF”, “O1_TF” and “O2_TF” were composed of TFs with different architecture. The analysis was also extended to those TFs that targeted the seven protein-coding genes with high expression in ripe fruit (“Cluster”, Figure 4, panel (c)).

Supplementary Files

This is a list of supplementary files associated with this preprint. Click to download.

- SuppFig2s.tif
- SupplementaryTable120200305.xlsx
- Table1v8.pdf
- SupplementaryTable2.xlsx
- SuppFig1.tif

- SupplFig3.tif
- SupplFig4.tif